EIGHTH EUROPEAN ROTORCRAFT FORUM

Paper No: 2.12

AERODYNAMICS OF THE HELICOPTER REAR FUSELAGE UPSWEEP

J. SEDDON

CONSULTANT, WESTLAND HELICOPTERS

AND UNIVERSITY OF BRISTOL

August 31 through September 3, 1982

AIX-EN-PROVENCE, FRANCE

ASSOCIATION AERONAUTIQUE ET ASTRONAUTIQUE DE FRANCE

AERODYNAMICS OF THE HELICOPTER REAR FUSELAGE UPSWEEP

J. SEDDON

Consultant, Westland Helicopters and University of Bristol

Summary

It is established that two very different types of flow can exist around the bluff upswept rear fuselage typical of some helicopters; and the change from one type (eddy flow) to the other (vortex flow) can, depending on the circumstances, be accompanied by a large increase in drag and a reduction in fin effectiveness. Angle of incidence of the fuselage (α) is an important parameter, as are lateral taper and to a lesser extent edge radii. Results are presented for two series of rear fuselage shapes, each covering a range of upsweep angles (ϕ). The nature of the vortex type flow is discussed. An $\alpha\phi$ diagram provides a useful way of assessing a given type of configuration from a design aspect. In a final section the two types of flow are put into a broader context by means of an extended $\alpha\phi$ diagram.

---

1. Introduction

Experience on fixed-wing aircraft has shown that where a rear fuselage shape is necessarily bluff, as for example when rear loading doors are required, the prediction of fuselage drag is exceptionally uncertain; and this uncertainty relates to a failure to understand sufficiently well the nature of the flow separations that occur. A case in point was that of the Short Belfast[1]: through this and other experiences it has become apparent that rear-end drag can in some circumstances be higher than would correspond to classical bluff-body separation.

New light has been thrown on this situation by work done in recent years (refs. 2-5 *et al*) on the drag of slanted bases, with particular reference to the design of hatch-back cars. T. Morel in particular has shown[4] that the flow over a slanted bluff base takes either of two forms, depending on the angle of slant; the one form a classical bluff body separation with standing eddy, the other a flow characterised by two streamwise vortices, after the manner of the flow over a slender wing at incidence, a type of flow nowadays well established[6] in the aeronautical field. Eddy flow exists at large slant angles; as slant angle is decreased a critical value is reached at which the flow changes suddenly to the vortex type and this change causes an immediate large increase in drag. Further decrease of slant angle is accompanied by a progressive decrease in drag, ultimately to levels below those associated with the eddy flow.

The present investigation has the objective of putting these aerodynamic phenomena into the context of helicopter design, for cases where a bluff rear fuselage upsweep is a practical feature. There are obvious environmental differences to the problem, as between the helicopter and the hatch-back car, notably the addition of a flight incidence range for the helicopter. The interaction of angle of incidence and slant angle (hereinafter termed upsweep angle) requires exploration *ab initio*. This paper gives an account of research carried out at the University of Bristol during the past three years. References 7, 8 contain the detail of undergraduate student experiments. The paper reviews these and presents the results of further experiment and analysis by the present author.

2. Description of experiments

The experiments were made in the Aeronautical Engineering Department's 7 ft x 5 ft low speed wind tunnel. A 1/5 scale model of an early version of the Lynx was used as a basis, on to which the required rear-end shapes were built (Fig.1,2). Two series of shapes have been investigated (1) with parallel-sided rear fuselage ("untapered bases") and (2) with laterally-tapered rear fuselage ("tapered bases"). A range of upsweep angles of the base was covered in each case. Series (1) had sharp edges at the base: series (2) had moderately rounded edges but at one upsweep angle a sharp-edged version was also tested.

Concerning limitations, the Reynolds number of the tests was of course low; but the boundary layer was always turbulent before reaching the base and therefore the separation phenomena would not be expected to be significantly Reynolds number sensitive. Morel's work covered this point experimentally and arrived at the same conclusion. More significantly, perhaps, the model had no rotor, nor was rotor downwash simulated in any way. Comment is made in the paper on the qualification this introduces into the results.

3. Results with untapered bases

A typical variation of drag with incidence in the mid-range of upsweep angles (40°) is shown in Fig. 3. As incidence is decreased (nose going downwards) a point is reached at which the level of drag increases suddenly. Surface pressure plotting on the base and wool tuft surveys show that this critical point corresponds to a sudden change from eddy flow to vortex flow. An indication of the stability of each of the two flow regimes is the occurrence of hysteresis to the extent of about 5° in critical incidence. Incremental drag due to the bluff base is obtained by comparing the measured drag with that for the basic model (both measurements inclusive of model supports), the latter being effectively a streamlined shape.

In Fig. 4 the results of Mistry and Lamb[7] are plotted in the form of drag against upsweep angle at constant incidence (nose going downwards). This corresponds to the typical presentation of Morel for hatch-back cars (one incidence only) and exhibits essentially the same features. Taking any one variation at constant incidence, eddy flow shows a minimum drag at 90° upsweep (vertical base) and a modest increase as upsweep angle is reduced. Vortex flow, established at the critical point, shows an immediate high drag followed by a falling characteristic as upsweep angle is further reduced.

There are here two features of concern to the helicopter designer (1) the critical flow change which, coming in at a particular incidence (Fig. 3), is potentially undesirable for aircraft flying control and (2) the high drag in vortex flow which persists for a significant range of upsweep angles below the critical.

Fig. 4 shows that the amount of drag rise at the critical is strongly a function of fuselage incidence. At sufficiently negative incidence it can be enormous: at -9° incidence with 40° upsweep (the case shown in Fig. 3) the drag jump itself is equal to about 70% of the drag of the basic model (effectively a streamlined shape) plus its supports: on a conservative reckoning of support drag, this means that the magnitude of the jump is about twice the basic fuselage drag.

4. Results with tapered bases

Fig. 5 gives the drag measurements for the series of tapered bases with moderately rounded edges, plotted against incidence as in Fig. 3. Here a

discrete drag jump is observable in only one case (60° upsweep). This is not to say that no flow change occurs for the other angles but only that drag changes are smaller than for the untapered bases. As concerns the type of flow, the results at positive incidence suggest that the flow here is of eddy type for upsweep angles 40°, 47° and 60° and of vortex type for 31° only. This difference in drag characteristics at positive incidence is equally a feature of the untapered bases, though not included in Fig. 3 (see however Fig. 9). It would follow, therefore, that a flow change occurs with each of the first three upsweep angles but not with the last.

To check this out more firmly, we resort to the surface pressure distributions. Typical chordwise pressure distributions on the base are shown in Fig. 6 for both untapered and tapered bases. The untapered base result shows the essentially different characteristics produced by eddy flow and vortex flow; in the former case an almost constant pressure, in the latter case a higher suction at the start of the upsweep and a more strongly varying distribution. These characteristics can also be seen clearly in the tapered base results and together with the further support of tuft flow observations, they provide definitive evidence on the type of flow existing. From this evidence, an approximate boundary between eddy flow and vortex flow can be defined (Fig. 7) and the variation of drag with upsweep angle constructed (Fig. 8), using Fig. 4 as a pattern.

It is seen from Fig. 8 that the critical upsweep angles are significantly higher for the tapered bases than for the untapered ones, for example at -14° incidence, 60° upsweep compared with 45°. Drag changes are generally much smaller than with untapered bases but the drag jump, where it occurs, is nevertheless still significant by comparison with the basic fuselage drag. Coupled with the movement in critical upsweep angle, however, the significant drag jumps occur at more extreme negative incidences.

Incremental drag attributable to both untapered and tapered bases is shown in Fig. 9. This is obtained as the excess drag over that of the basic model at the same incidence, expressed as a coefficient in terms of the projected area of the base. The latter is the same for all models of a series but different for untapered and tapered bases by a factor approximately 2:1.

5. $\alpha\phi$ diagrams

Up to this point, the emphasis has been on showing that the upswept rear fuselage of a helicopter can, within a range of upsweep angles, produce either of two discrete types of flow, which in turn may have significantly different drag characteristics. The situation for a given case is summarised in a plot of upsweep angle ϕ against angle of incidence of the fuselage α: in this diagram is shown the locus of critical points, or critical boundary, separating eddy flow and vortex flow, together with suitably defined excess drag zones. Such $\alpha\phi$ diagrams for the untapered and tapered bases are presented in Figs. 10, 11. Points to note include the following:-

(a) For untapered bases, the critical range of upsweep angles is from 33° to 51° approximately. Below the former the flow cannot be of eddy type; above the latter it cannot be of vortex type. The corresponding angles for tapered bases are 35° and 70° approximately.

(b) The boundary for untapered bases is that derived from Fig. 4 and represents the changeover points when incidence is decreasing. The single measurement of hysteresis shown in Fig. 3 suggests that for incidence increasing the boundary would shift to more positive incidences, by about 5° at 40° upsweep, probably zero at 33° upsweep and perhaps 10° at 50° upsweep. No hysteresis was detected in the tests of tapered bases.

(c) The important excess drag zone is that at negative incidences and below the critical boundary. Here the high drag arises from suction on the base associated with vortex flow. This zone is defined in the $\alpha\phi$ diagrams by the range of upsweep angles below the critical for which the drag remains above the level corresponding to eddy flow at the critical point. In Figs. 10, 11 the excess drag zones are shaded progressively to indicate low, moderate, high and very high excess drag (only the first two exist in Fig. 11). For more explicit indication of the amount of excess drag, reference is made back to Figs. 4, 8.

(d) For incidences above the minimum drag point, the drag in eddy flow is always higher than that in vortex flow. This applies to both series of bases and can be seen exemplified in Fig. 4 (curve for $\alpha = +9^{\circ}$) and more clearly in Fig. 9. A second excess drag zone is thereby defined, in this case on the eddy flow side of the critical boundary.

(e) Using Fig. 10 as presented, it would be concluded that for flight at -9° incidence, the upsweep angle should be either above 40° or below 20° (for zero excess drag) or 28° (for only small excess drag).

6. Vortex flow and the incidence effect

It is clear from the evidence that the occurrence of vortex flow in the helicopter context is strongly incidence-related. At zero incidence the drag jump is relatively small, even for the untapered bases (Fig. 4). It is not clear why this should be so in view of the hatch-back car evidence which is essentially for a "zero-incidence" case: however, the sensitivity is such that by -3° incidence (Fig. 4) the jump appears to be of similar magnitude to those in Morel's work.

A second feature is that as incidence decreases, the critical upsweep angle increases. One might from first principles have expected an opposite trend, whereby for the critical change the upswept base would be at a certain angle to the free stream, implying a relationship,

$$\phi - \alpha = \text{constant}.$$

That this is not the case points to the importance of the angle between flow along the bottom of the fuselage (approaching the upsweep) which is at inclination α to the free stream, and that along the side of the fuselage, which is more nearly in line with the free stream. It seems that this angle has the double effect (a) of delaying the point at which, as incidence is decreased, the flow along the bottom of the fuselage can turn up the base and (b) when this point is reached, of strengthening the attendant vortices, leading thereby to the result that the larger the upsweep angle, the greater is the drag jump when it occurs. In practical terms, these points are well demonstrated in the $\alpha\phi$ diagram (Fig. 10) which shows the increase of critical upsweep angle as incidence is increased negatively (in fact, for negative incidences the boundary is reasonably close to a straight line, $\phi+\alpha$ = constant) and also the concentration of high vortex-flow drag towards the higher negative incidences.

7. Lateral taper and edge radii

The less dramatic results shown with the tapered bases are accounted for by the combined effect of lateral taper of the fuselage and rounding of the edges of the base. Considering first the edge rounding, an additional test was made with a sharp-edged version of the 47° upsweep model. Comparing results, the sharp-edged model gave appreciably the higher drag at positive incidences: this is where the flow is of eddy type and clearly, with sharp

edges the flow separations are fixed in a way which maximises the size of the eddy flow region, so a higher drag is not unexpected. At negative incidence, where the flow has changed to vortex type, the drags of the two versions were approximately the same. The most significant evidence was provided by the pressure distributions, which indicated that the critical changeover occurred at a more negative incidence with the sharp edges; in other words, at constant incidence the change would occur at a lower upsweep angle (perhaps by 4°). The rounding therefore accounts for some (perhaps one-third) of the shift in position of the critical boundary as between Figs. 10 and 11. The result is in agreement with Morel's findings[4].

The more major change is that resulting from lateral taper. There are various ways of looking at the effect. One might say that lateral taper near the top of the fuselage allows air to be vented directly into the base flow region, thereby inhibiting development of the vortices emanating from lower down the base. Alternatively using the slender wing analogy (section 1), the base plan form is now like a slender wing operating in reverse, i.e. with the widest part at the front: this would certainly have a weakening effect on vortex development.

8. Fin effectiveness

Hinchcliffe and Westland[8] found that the existence of vortex flow had a detrimental effect on the restoring moment in yaw of a vertical fin mounted on top of the tail boom. Some results are given in Fig. 12. Plotted vertically is a measure of fin effectiveness, defined as the difference in slopes of yawing moment against angle of yaw for the model with fin on and fin off, the slopes being taken at zero yaw angle. Plotting this quantity against negative incidence for several models gives the results shown. With 60° upsweep, giving eddy type flow throughout the incidence range, the fin is consistently effective. With 46° and 40° upsweep, however, the effectiveness at zero incidence is of the same order as for 60° upsweep, but when the flow changes to vortex type at the critical incidence, the effectiveness falls suddenly and is even negative for a time. The mechanism of low fin effectiveness is probably that suggested in the accompanying sketch, whereby a differential strength in the two vortices gives rise to a cross-flow at the fin position in the destabilizing sense.

9. Note on rotor simulation

All the experiments to date have lacked any simulation of rotor flow. Inclusion of rotor downwash, increasing as flight speed diminishes i.e. as incidence increases, would have the effect of elongating the $\alpha\phi$ diagram progressively towards the more positive incidences. In other words, the incidence for changeover would be increased by the effect of downflow on the sides of the fuselage, bringing the changeover, and possible high vortex-flow drag, more into the flight regime. A similar effect was present on the Short Belfast[1] from the downwash of a high wing set at incidence to the fuselage.

10. The extended $\alpha\phi$ diagram

In this general account of base flow situations, it is pertinent to ask two questions:

(1) Why does the critical boundary have the particular shape shown in Figs. 10, 11?

(2) How do the two types of flow discussed relate to a third type, namely streamlined flow, which is the normal target of aerodynamic design?

A first clue to answers is provided by the way that both the experimentally-derived boundaries turn upwards at positive incidence. For any upsweep angle, it

may be presumed that as positive incidence is increased, a point will be reached at which the inclination of the base to the line of flight (the horizontal) becomes so small that there is no flow separation on the base itself. The base is now effectively in streamlined flow. General considerations of streamlining lead to the expectation that this will happen when the angle of the base to the horizontal is down to about 20°, i.e.

$$\phi - \alpha \simeq 20^{\circ}$$

This approximate boundary can be added to the $\alpha\phi$ diagram and is readily seen to provide a plausible extension of the upturn of the experimental boundaries at positive incidence.

At the negative incidence end, there would appear to be a natural limit to the existence of vortex flow when the upswept surface reaches the vertical. Beyond this the vortices would be required to develop in a direction opposing the mainstream on the fuselage sides. This limit is defined by

$$\phi - \alpha \simeq 90^{\circ}$$

and again a plausible extension of the critical boundaries is provided.

The total picture thus constructed is presented in an extended $\alpha\phi$ diagram (Fig. 13) which shows the juxtaposition of all the three possible types of flow. We take a series of sweeps at constant incidence through the diagram. Starting with streamlined flow, as upsweep angle is increased this changes directly into eddy flow if the incidence is greater than about 5°. For a lower incidence, however, streamlined flow will first change into vortex flow, which then at higher upsweep angle is transformed into eddy flow. For still lower incidence, streamlined flow is not possible and we have vortex flow at low upsweep angle changing into eddy flow at higher values. The experimental boundary thus appears as a transition line reaching across between natural boundaries B1 and B2. Given in addition that the larger the negative incidence, the stronger is the "starting vorticity" provided by the angle between flow on the bottom of the fuselage and that on the side (this has been argued in section 6), the general shape of the experimental boundaries is fully accounted for.

11. Conclusions

(1) It has been established that two very different types of flow can exist around the bluff upswept rear fuselage which is a feature of some helicopters; and the change from one type (eddy flow) to the other (vortex flow) can, depending on the circumstances, be accompanied by a large increase in drag and a reduction in fin effectiveness.

(2) The nature of vortex type flow is discussed at some length. Primary parameters are upsweep angle, ϕ, and angle of incidence of the fuselage, α, and an $\alpha\phi$ diagram provides a useful way of assessing a given configuration from a design aspect.

(3) For a series of untapered bases as tested, upsweep angles below 33° produce only vortex type flow and those above 50° only eddy type flow. For intermediate upsweep angles both flows exist, the point of changeover depending on angle of incidence, with some hysteresis.

(4) When the changeover to vortex flow occurs, at negative incidence, there is an immediate increase in drag caused by high suction on the base associated with the vortex formation. The drag jump can be very large, typically about twice the basic fuselage drag.

(5) Onset of the vortex flow can also cause a sudden reduction of fin effectiveness, the differential strength of the two vortices in yawed flow leading to a net cross-flow at the fin in a destabilizing sense.

(6) For a series of tapered bases - corresponding to lateral taper of the rear fuselage - the flow changeover is still detectable but the result is less dramatic in a drag sense. For a given incidence the critical upsweep angle is higher than for untapered bases. Only at high negative incidence and high upsweep angle (e.g. $\alpha = -14^{\circ}$, $\phi = 60^{\circ}$) is a significant drag jump found. Tail surface power may be affected more widely but this has not been investigated.

(7) Lateral taper accounts for most of the difference in severity of the effects found with the two series of bases but a change was made from sharp to rounded edges at the same time and from a single check it appears that edge radius is also a factor. Further experiments are required if these two factors are to be separated. Also, different forms of lateral taper could produce different results.

(8) In a final section of the paper, the two types of flow, eddy flow and vortex flow, are put into a more complete context by use of an extended $\alpha\phi$ diagram. This brings in the one other type of flow which could be envisaged as applying to the rear fuselage design, namely streamlined flow, under which no flow separation would occur forward of the extreme point of the base. It also introduces the concept of an upper limit to vortex flow, namely when the upswept base reaches a vertical position relative to the line of flight.

Notation

α angle of incidence of fuselage to wind (+ve nose up)

ϕ angle of upsweep of base surface relative to bottom of fuselage

D drag force

C_D drag coefficient = D/qS

q free stream dynamic head = $\frac{1}{2}\rho V^2$

ρ density of air

V free stream velocity

S a reference area, either cross-sectional area of fuselage or projected area of base, as required

C_p pressure coefficient = $\dfrac{\text{(local static pressure - free stream static pressure)}}{\frac{1}{2}\rho V^2}$

x distance along base slant from start of upsweep

c total distance (chord) along base slant

References

1. B.G. Lowe and W.J.G. Trebble; Drag analysis on the Short SC5 Belfast; Unpublished Royal Aircraft Establishment Report, 1968

2. L.J. Janssen and W.H. Hucho; Aerodynamische Formoptimierung der Type VW-Golf and VW-Scirocco; Kolloquium über Industrie - aerodynamik, Aachen, Part 3, pp. 46-49, 1974

3. T. Morel; The effect of base slant on the flow pattern and drag of 3-D bodies with blunt ends; G M Res. Lab. Symposium Sept 1976

4. T. Morel; Aerodynamic drag of bluff body shapes characteristic of hatch-back cars; SAE Congress and Exposition, Detroit 1978

5. P.W. Bearman; Bluff body flows applicable to vehicle aerodynamics; ASME - CSME Conference, Niagara Falls, 1979

6. D. Küchemann; The aerodynamic design of aircraft, Chapter 3, pp.69-71; Pergamon Press, 1978

7. H. Mistry and R. Lamb; An investigation of drag associated with the upswept rear fueselage of a helicopter; University of Bristol, Aero Engineering Report No. 257, 1980

8. R.A. Hinchcliffe and P.G. Westland; The effect of sideslip on the vortices shed from the upswept rear fuselage of a helicopter; University of Bristol, Aero Engineering Report No. 267, 1981

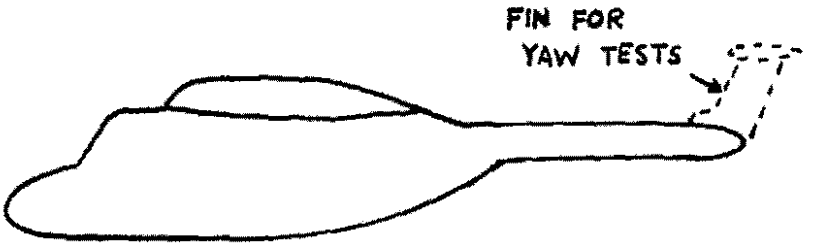

FIG 1 : BASIC MODEL

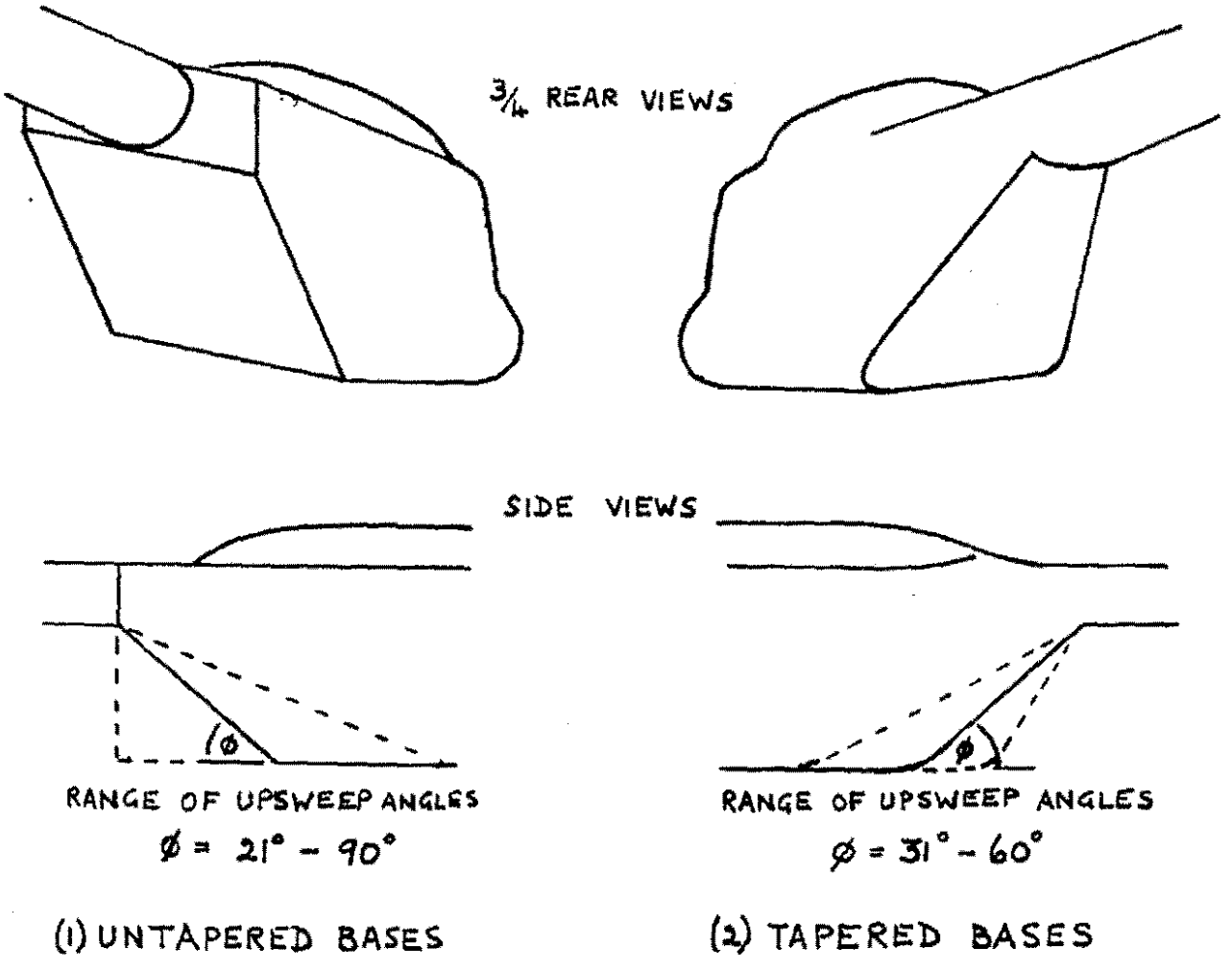

FIG 2 : MODEL SERIES (1) AND (2)

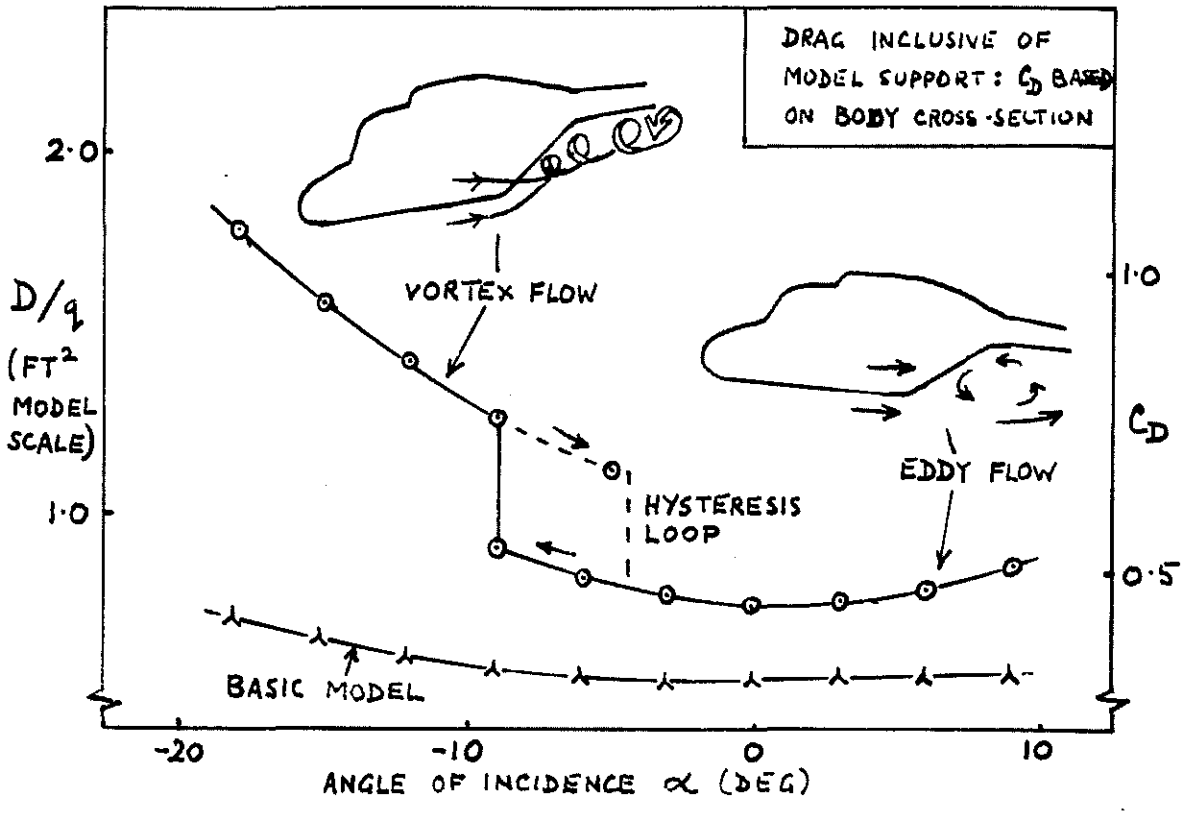

FIG 3: TYPICAL DRAG VARIATION FOR UNTAPERED BASE
(UPSWEEP ANGLE 40° ; RESULT FROM REF. 7)

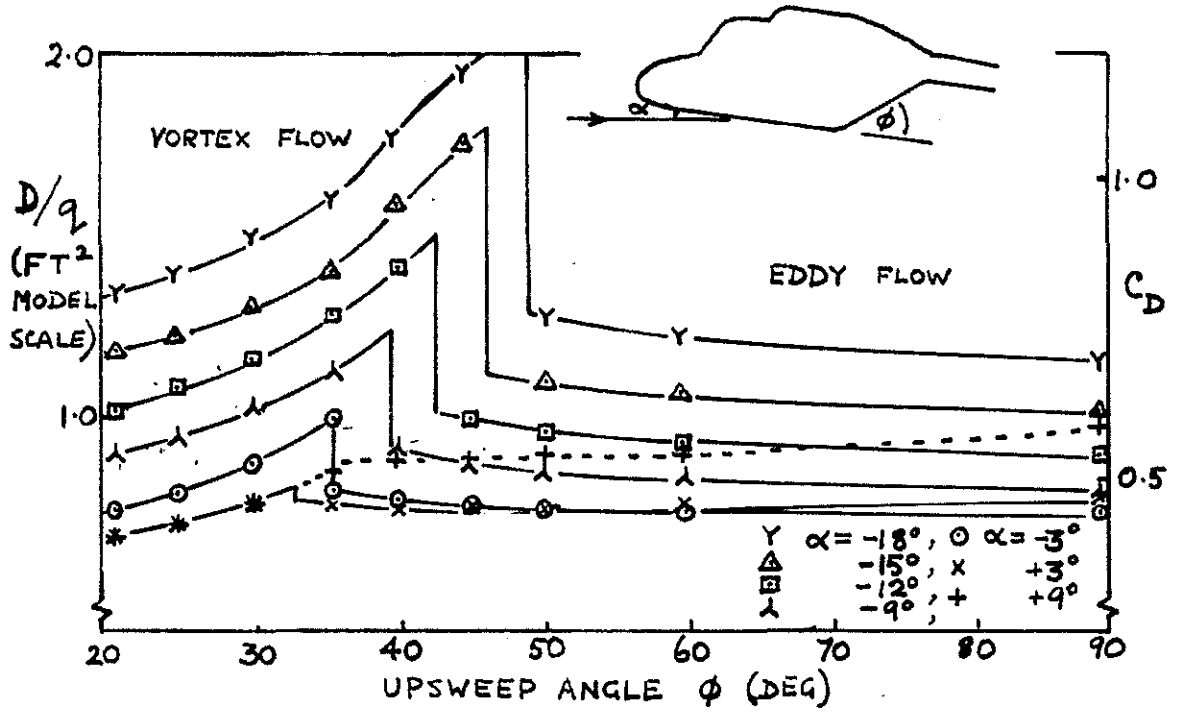

FIG 4: VARIATION OF DRAG WITH UPSWEEP ANGLE AT CONSTANT INCIDENCE FOR UNTAPERED BASES (RESULTS OF REF. 7)

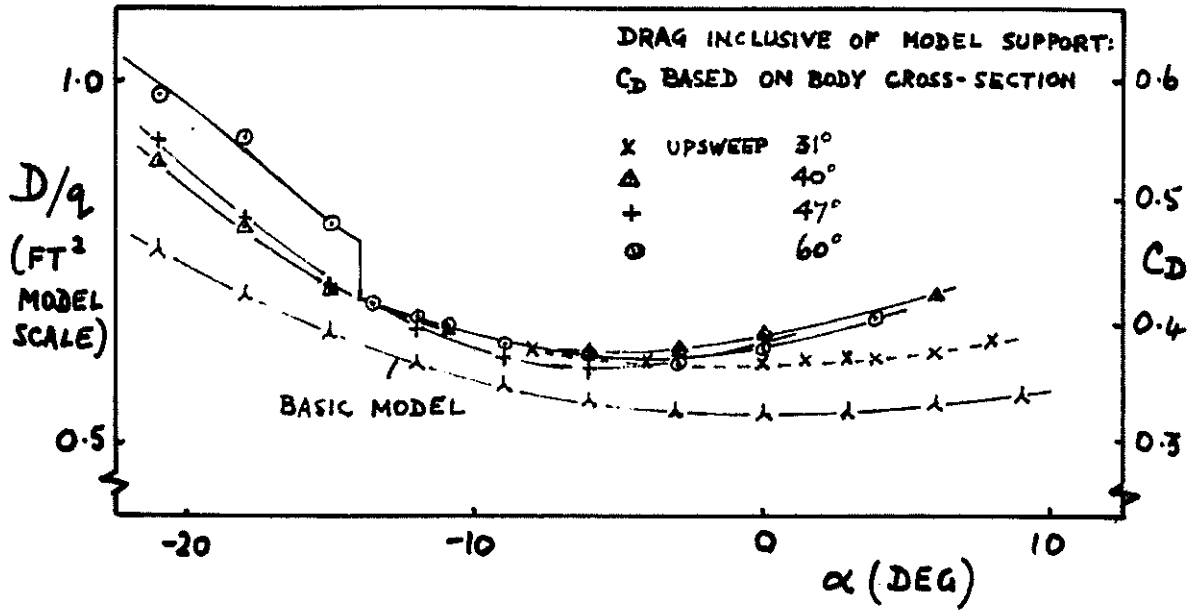

FIG. 5: DRAG VARIATION FOR TAPERED BASES

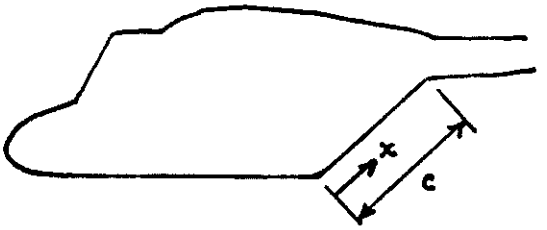

C_p IS MEAN SPANWISE PRESSURE COEFFICIENT AT CHORDWISE x.

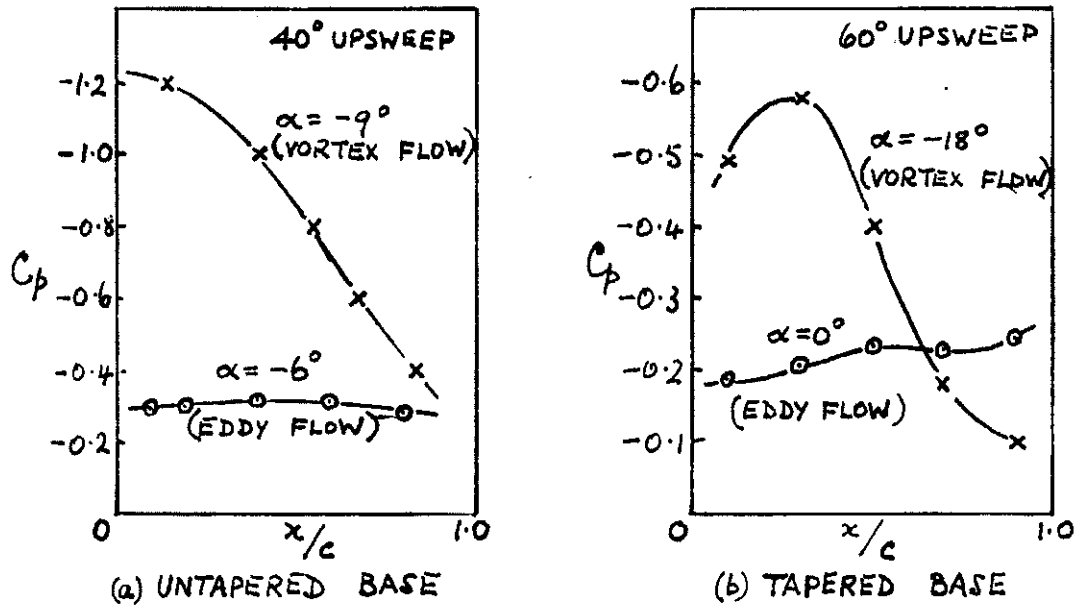

(a) UNTAPERED BASE (b) TAPERED BASE

FIG. 6: TYPES OF PRESSURE DISTRIBUTION

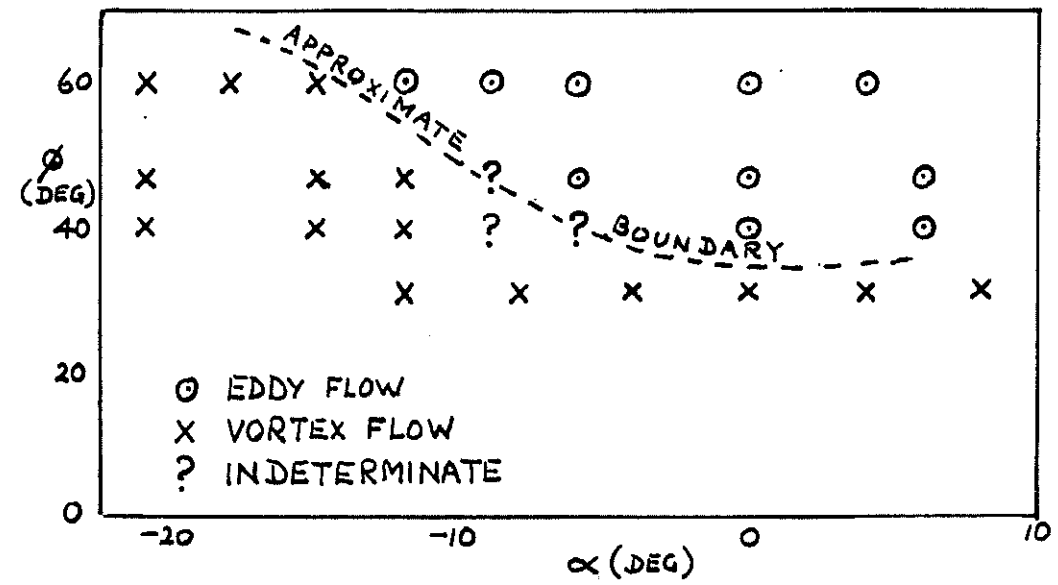

FIG. 7: DETERMINATION OF BOUNDARY FROM PRESSURE DISTRIBUTIONS : TAPERED BASES

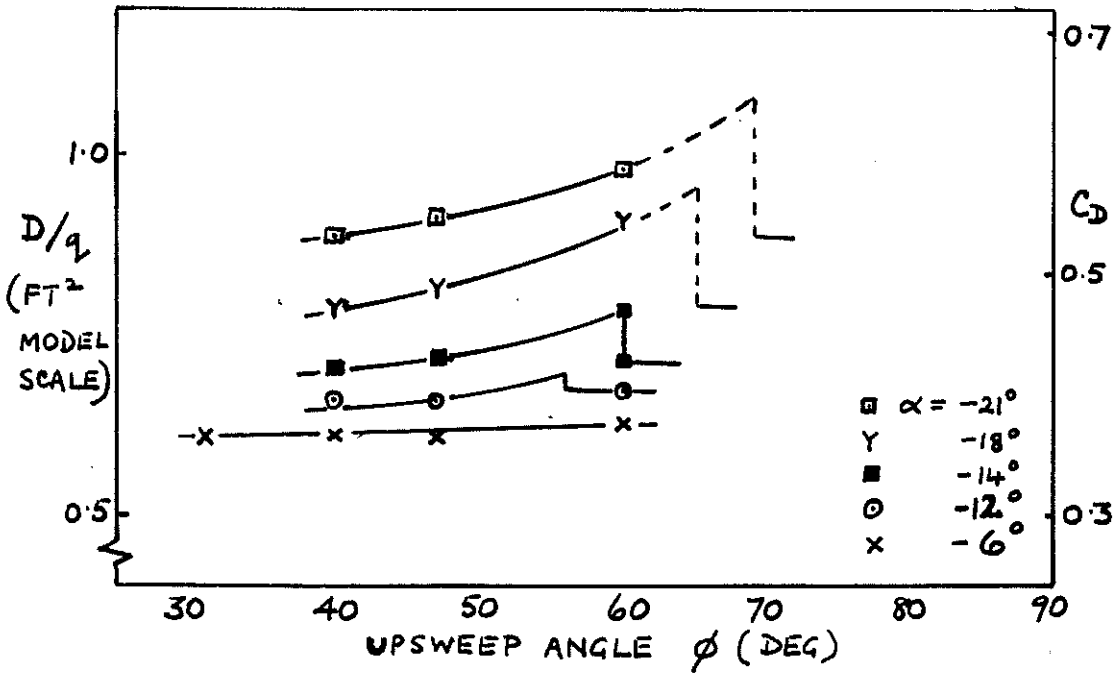

FIG. 8: DRAG VARIATION WITH UPSWEEP ANGLE AT CONSTANT ∝ : TAPERED BASES

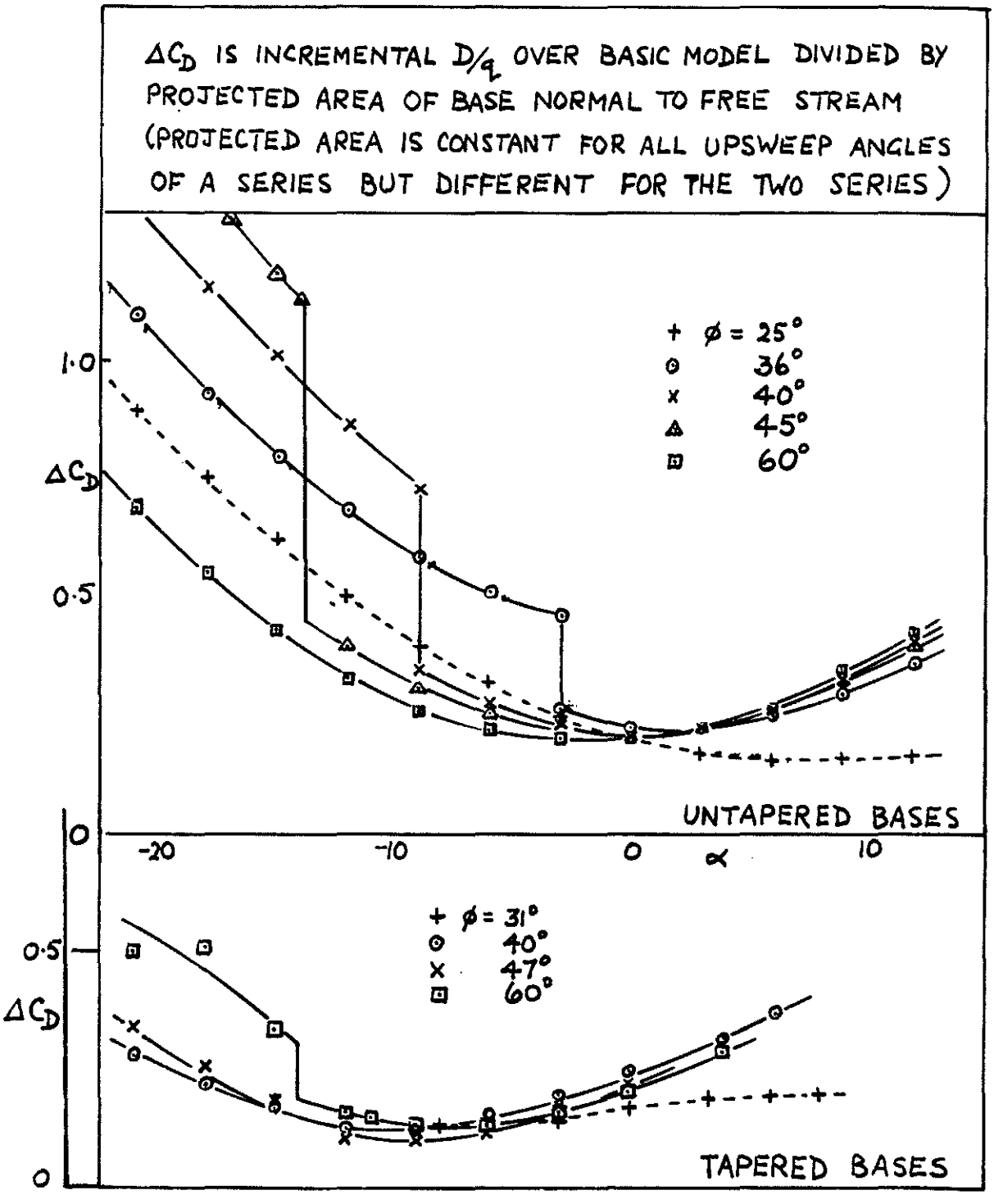

FIG 9 : DRAG INCREMENT ATTRIBUTABLE TO BLUFF BASES

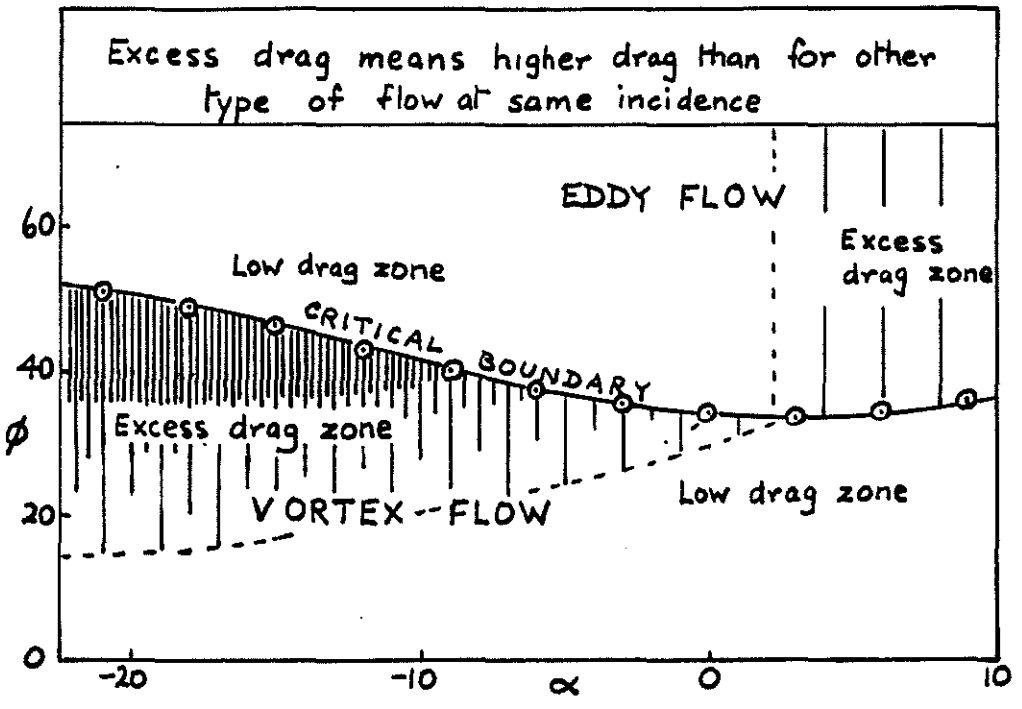

FIG 10: $\alpha\phi$ DIAGRAM FOR UNTAPERED BASES

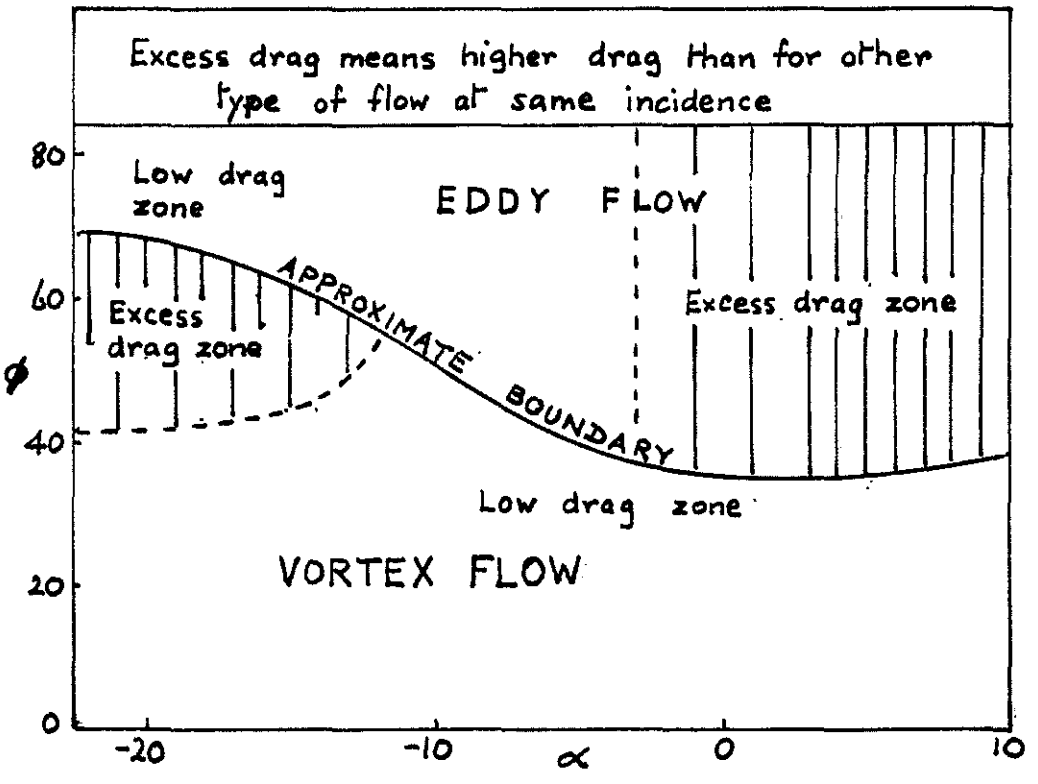

FIG 11: $\alpha\phi$ DIAGRAM FOR TAPERED BASES

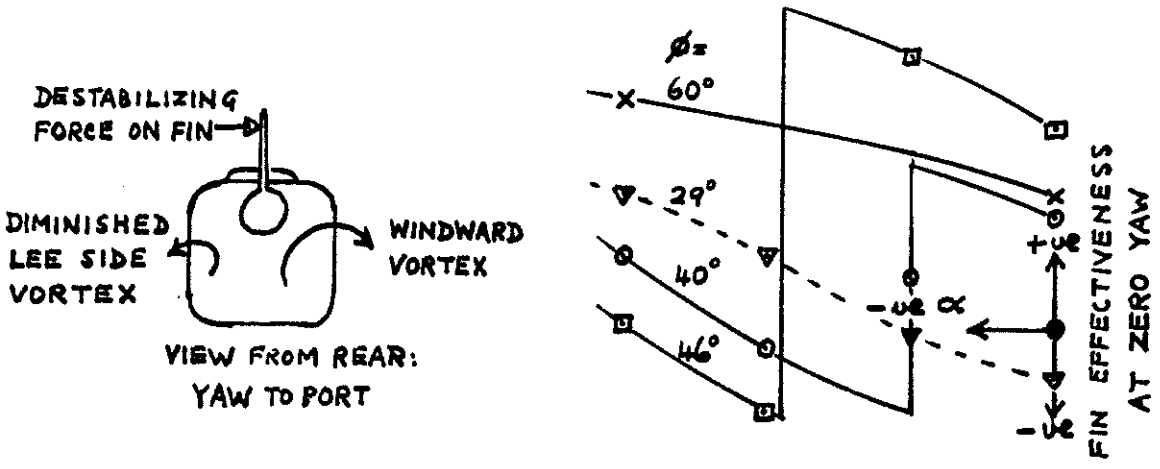

FIG 12: FIN EFFECTIVENESS WITH UNTAPERED BASES (RESULTS OF REF 8)

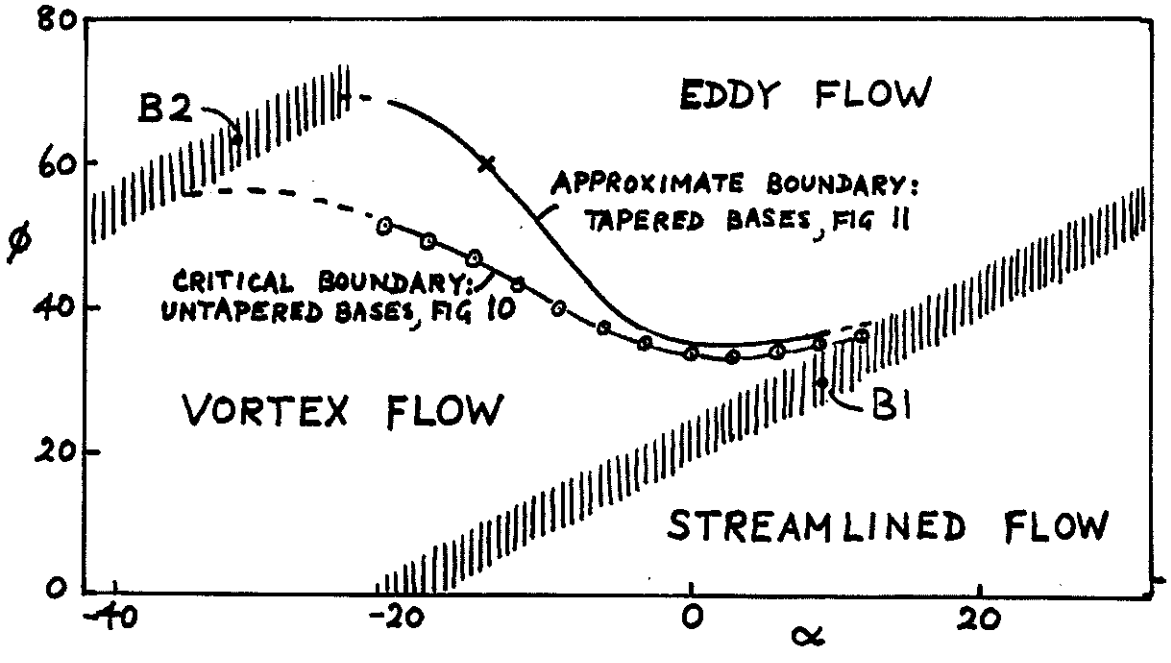

FIG. 13: THE EXTENDED $\alpha\phi$ DIAGRAM